5 Holocene climate evolution of the Ugii Nuur basin, Mongolia

Schwanghart, W., Schütt, B., Walther, M. (2008). *Advances in Atmospheric Sciences*, 25, 6, 986-998.

Summary

In order to evaluate the Holocene palaeoenvironmental evolution of the Ugii Nuur basin, central Mongolia, investigations on chemical and mineralogical properties of lacustrine sediments were carried out on a 630 cm long sediment core of lake Ugii Nuur. The interpretation of the record is based on a principal component analysis (PCA) of the elemental composition of the samples. The results show that lacustrine deposition started at 10.6 ky BP. Low lake level conditions were identified during the Early Holocene (10.6–7.9 ky BP). The Mid Holocene (7.9–4.2 ky BP) was characterized by generally higher lake levels and thus moisture supply, but experienced strong climatic fluctuations. Arid conditions prevailed from 4.2–2.8 ky BP and were followed by a stable, more humid phase until today.

Keywords

lake sediments, palaeoclimate, Central Asia, Mongolia, Holocene

5.1 Introduction

Moisture availability is one of the most important natural factors governing almost all aspects of societal and economical life. In East and Central Asia moisture supply is mainly attributed to the Indian and South-East Asian Monsoon. These wind systems are highly variable in space and time driven by interactions between global atmosphere, ocean, land and ice systems as well as conditions imposed by the concurrence of the East Asian land mass and solar radiation (An, 2000).

A key to the understanding of the complex controls on these wind systems are records of climate change that are accessed and interpreted by palaeoenvironmental research. A large number of studies on the Chinese loess sequences (e.g. Maher and Thomson, 1991; Madsen *et al.*, 1998; Fang *et al.*, 1999; Zhu *et al.*, 2004; Liu *et al.*, 2005), lake systems (e.g. Walther *et al.*, 2003; Wünnemann *et al.*, 2005; Prokopenko *et al.*, 2007), ice cores (e.g. Thompson *et al.*, 1997; Yao *et al.*, 1997) and speleothems (e.g. Wang *et al.*, 2001) have provided insight into the climatic and environmental evolution of the regions affected by monsoon variability and, thus, increased the understanding of their sensitivity to climatic change.

Moreover, current research on the human dimension of monsoon variability increased the understanding of climate and human interactions in monsoonal Asia (Rost *et al.*, 2003; An *et al.*, 2005; Fu and de Vries, 2006; Yancheva *et al.*, 2007). This issue becomes particularly challenging when considering the environmental changes and problems that monsoonal Asia faces especially in its arid and semi-arid regions and that are likely to increase in the future driven by climate change (Liu and Diamond, 2005).

An understanding of the prehistorical and historical climate and human interactions in central Mongolia is the aim of ongoing research conducted by archaeologists from University of Bonn (Germany) and geographers from Freie Universität Berlin (Germany). Their research focusses on the Orkhon Valley that has experienced a vicissitudinous history of human influence (Rösch *et al.*, 2005) since various cultures preferred this region as settlement location due to its strategic position (Bemmann *et al.*, 2008). Moreover, its situation in the semi-arid steppe region makes it highly vulnerable to climate change (Gunin *et al.*, 1999; Tarasov *et al.*, 1999b; Dulamsuren *et al.*, 2005a).

Since the climatic forces, their variability and the environmental history of this region are still poorly understood, this paper addresses the paleoenvironmental history of the Ugii Nuur basin in the Orkhon Valley during the Holocene. We accomplish this goal by analyzing a lake sediment core spanning the entire Holocene history of Lake Ugii Nuur. The interpretation is based on chemical and mineralogical properties of the lake sediments.

5.2 Regional setting

Lake Ugii Nuur is located at 47°44'N and 102°46'E at an elevation of 1328 m EGM96 (see Fig. 5.1). The freshwater lake has a surface area of ca. 26 km^2 and a maximum depth of 16 m. Presently, the lake is described as a thermally stratified, oligo- to mesotrophic, dimictic lake with a visible depth of 7.3 m. The metalimnion is found between 10 and 12 m above an unstable hypolimnion (Völker, 2005). The lake basin opens towards the 12–20 km wide Orkhon valley in the western part of the catchment. The Old Orkhon River (*Chögschin Gol*) constitutes the inlet in the western part of the lake. This perennial river drains an area of 4655 km^2 that includes the eastern branches of the Khangay Mountains. The outlet is located northwest to the inlet and joins the Orkhon River after a distance of 7 km (Fig. 1). This water course is only ephemerally active due to overflow from Ugii Nuur. During the two field campaigns in summer 2005 and 2006 it was dried out or marshy.

While terrain in the southern and eastern drainage basin is characterized by undulating relief, the northern part is hilly to mountainous with elevations up to 1600 m. Bedrock in the basin consists to a large extent of aeolian silts and fine sands covering Carboniferous shists and shales that outcrop along ridges and steep slopes (Schwanghart and Schütt, 2008). Cliff lines along the southern and eastern shore are partly composed of conglomerates of probably late Cretacious and Tertiary age (Traynor and Sladen, 1995; Sladen and Traynor, 2000). Soils are weakly developed and differentiated by Leptosols, Regosols and Kastanozems according to their position in the relief (Haase, 1983).

The Ugii Nuur basin is characterized by an extremely continental climate. Kharkhorin, a town located about 60 km south to Lake Ugii Nuur (Fig. 5.1), has a mean annual air temperature around zero and a yearly precipitation amount of approx. 290 mm (1962–1983). The continentality causes a strong seasonality in temperature and precipitation. Mean January air temperatures of −18.2°C contrast mean July air temperatures of 16.8°C. Highest precipitation rates generated by heavy rainfalls are found in summer, while precipitation in winter (November to March) mostly occurs in solid form and rarely exceeds 10 mm per month. The study site is situated within the area of dry, gras steppes (Hilbig, 1995; Opp and Hilbig, 2003) and is dominated by grasses (*Cleistogenes*, *Stipa*), forbs (*Allium*),

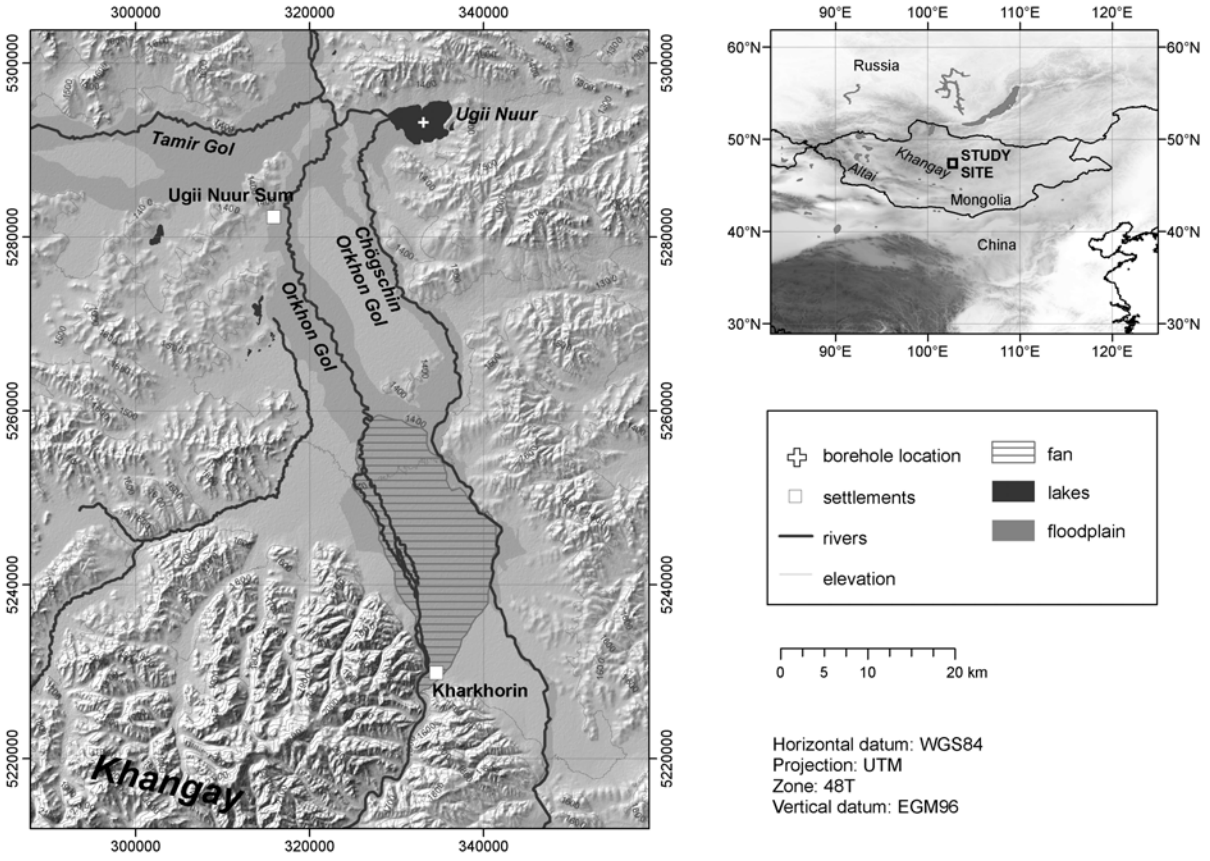

Figure 5.1: Map of the Ugii Nuur basin.

and shrubs (*Artemisia*, *Caragana*) while trees are generally lacking.

5.3 Methods

5.3.1 Sediment extraction and analysis

The sediment core Ugi-4 was drilled at the deepest point of Ugii Nuur in 2003 using a Usinger piston corer. The core has a length of 630 cm and was sampled with an interval of 10 cm and a resolution of 2 cm. Prior to chemical and mineralogical analysis the samples were dried at 50°C, screened on components larger 2 mm and homogenized in an agate disk swing mill (Lieb-Technik). We used a conductrometric carbon analyzer (Wöesthoff, detection limit = 0.02 mass-% C) to determine the total and inorganic carbon (TIC) content. Total organic carbon (TOC) content was calculated as the difference of both values. Mineralogical compounds were analysed by X-ray powder diffraction using a copper

k_α-tube (PW1729/40, Phillips) from $2\theta = 2$ to 52° and a step width of $2\theta = 0.01°2\theta$ with each step measured for one minute. Contents of mineral componenents were recorded semi-quantitatively (vol-%) using the software package Phillips X'Pert Highscore v. 1.0b (PW3209). After preparing samples using aqua regia and microwave digestion, we analyzed the element composition (Ca, Cr, Cu, Fe, K, Mg, Mn, Na, Ni, Pb, $P0_4$, S, Sr) by inductively coupled plasma atomic emission spectroscopy (ICP-AES, Optima 3000, Perkin Elmer).

5.3.2 Age control

Age control was established by AMS ^{14}C dating of three bulk sediment samples in 210, 510 and 580 cm depth by the Poznan Radiocarbon Laboratory. Since there is a lack of carbonatic rocks in the lake catchment we exclude an influx of old carbon skewing the $^{14}C/^{12}C$ ratio and, thus, the dates were not corrected for a reservoir effect. Calibration of radiocarbon dates was performed using CalPal, a software for calibration and visualization developed and distributed by the Prehistory Institute at University Cologne (http://www.calpal.de). As calibration curve CalPal2005-SFCP was used. All ages referred to hereafter are calibrated years unless otherwise noted.

5.3.3 Statistical analysis

We applied a principal component analysis (PCA) (Davis, 1986) based on the correlation matrix to reduce the complexity of the elemental composition of the samples. Since compositions only provide information on the relative magnitudes of the components and are subject to a constant sum constraint (CSC), interpretations involving absolute values may be biased (Aitchison, 1999; Aitchison and Egozcue, 2005). Aitchison (1986) presents a solution to the problem of applying multivariate statistics with CSC data by using *centered log-ratios*, that are linear combinations of the compositional variables. Log-ratios remove the negative bias in the covariance and correlation matrices introduced by the use of CSC data and avoid fallacious interpretations that emerge from raw component analysis (Kucera and Malmgren, 1998). The log-ratio of an observation i of a sample S is calculated by

$$y(i) = \ln(x(i)/g_s) \tag{5.1}$$

where g_s is the geometric mean of a sample calculated by

$$g_s = e^{(\ln x_1 + \ln x_2 + \cdots + \ln x_N)/N} \tag{5.2}$$

and N is the number of variables constituting the composition in the sample. The presence of zero elements requires a zero-replacement procedure that Aitchison (1986) implements by replacing all zero elements by a value lower than the precision under which the original data were generated (Kucera and Malmgren, 1998).

Prior to log-ratio transformation the unit of all chemical parameters was set to μg/g. Since our data does not add up to a constant sum (not all elements are determined by the aforementioned analysis techniques), the remaining proportion was included as additional variable, but was not included in the PCA.

In order to enhance the interpretability of the derived principal components (PCs) as real endmembers they were transformed using *Varimax* rotation. This orthogonal rotation generates an even distribution of variance on the PCs by maximizing the variance of the factor loadings. Geometrically, the factor loadings are the cosines between the variables and the factors and equal the correlation coefficient. For an interpretation of the factors 50% declared variance (modulus of factor loading > 0.7) was set as boundary value. The factor scores were estimated using regression in order to gain insight into the chronological behavior of the PCs.

5.4 Results

5.4.1 Sediment stratigraphy

The sediments of the core UGI-4 (Fig. 5.2) can be distinguished according to three major stratigraphical units characterized by fluvial sands at the bottom (section 12, 13), clayey to silty, organic rich sediments in sections 2-11 and organic poor loam in the overlying sediments (section 1, $<$ 140 cm). Sections 2-11 are mainly determined by alternating carbonate contents locally reaching calcite concentrations up to 30%. A fish scale found in the sediment core in 158-160 cm depth (sediment age of approx. 2800 y BP corresponding to the age model below) was identified by Joris Peters (LMU Munich) as remnant of a perch (*Perca sp.*), most likely *Perca fluviatilis*.

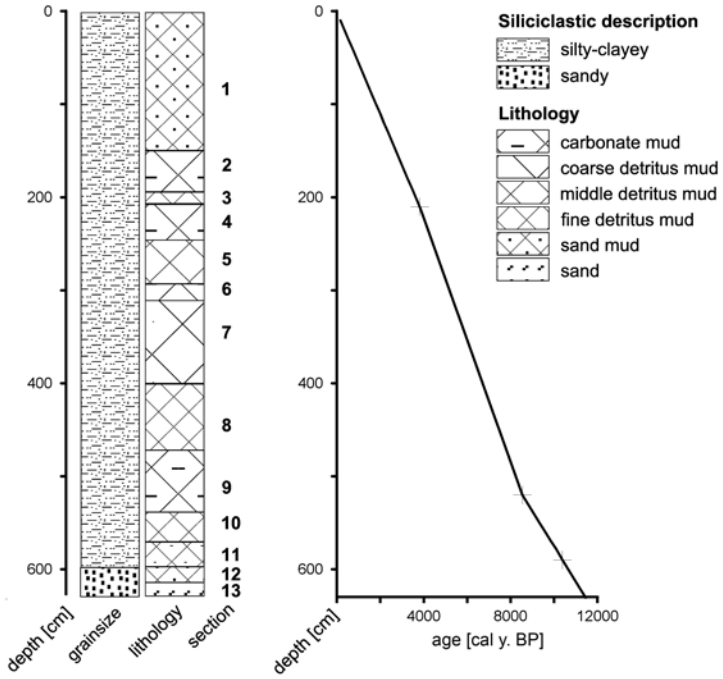

Figure 5.2: Lithography and age model of the core Ugi-4.

5.4.2 Age model

The AMS ^{14}C dates are 3535 ± 30 (Lab. no.: Poz-16767), 7770 ± 50 (Poz-16847) and 9210 ± 50 y BP (Poz-16768), respectively. Calibration of these dates yields 3809 ± 57, 8538 ± 55 and 10382 ± 84 cal. y BP. An age model was established by linear interpolation as displayed in Rig. 2. A linear extrapolation at the core end yields a sediment bottom age of 11400 y BP. Sedimentation rates derived from the linear interpolation range from 0.43 to 0.63 mm/y. Correspondingly, the sampling scheme of 10 cm intervals sampling rate and 2 cm resolution is to be equated with a sampling rate of 160–230 years, where each sample integrates over 31–46 years.

5.4.3 Element composition

Element compositions of the sediments are displayed in Fig. 5.3. Sequences of TIC, Ca, Mn and Sr feature various correlative peaks. TIC values range between the detection limit of 0.02 and 3.66 mass-%. Sections of increased TIC concentrations prevail from 530 to 468 cm and 220 to 158 cm depth. Further single peaks with amounts up to 2 mass-% are

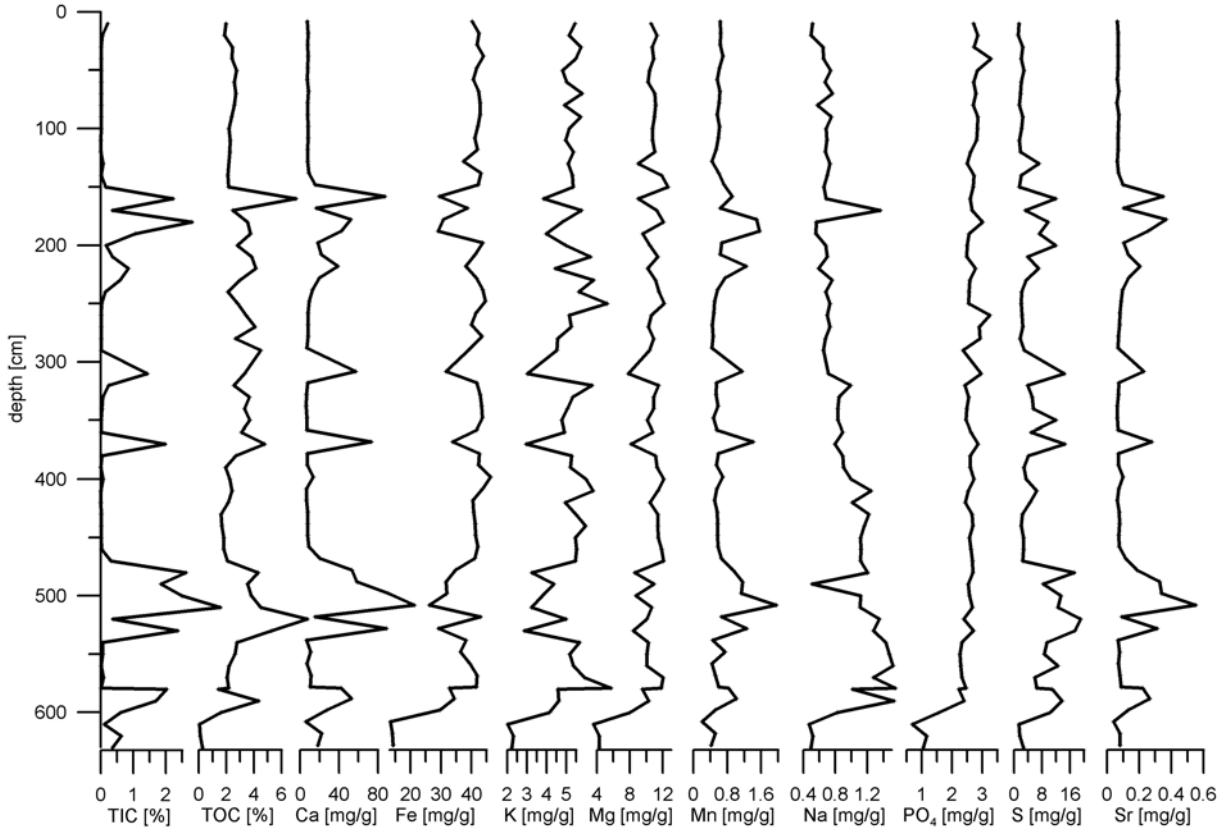

Figure 5.3: Element composition of Ugi-4.

found in 310, 370, 580 and 590 cm depth. Except for slightly increased TIC concentrations at the lake bottom, TIC content remains at the detection limit above 150 cm depth. Fe, K, Mg, Cr, Cu and Ni show a negative correlation with TIC and TIC-related elements (Fig. 5.3). Below 600 cm depth a sharp drop in concentrations coincides with change towards a different depositional environment as indicated by the lithography.

TOC concentrations range between 2 and 8 mass-% above 600 cm depth. Below 600 cm the concentrations rapidly decline below the detection limit. Peaks in TIC are partly associated with TOC increases. The TOC graph is characterized by distinct fluctuations throughout the profile. Coherent periods of low TOC values below 3 mass-% are found from 580 to 538 cm, 470 to 378 cm and above 150 cm. Some peaks of TOC overlap with increased sulphure concentrations. Here three distinct periods with notedly increased S concentrations are observed at 600 to 480 cm, 380 to 310 and 220 to 130 cm depth. Positive deflexions in TOC concentrations are frequently associated with negative peaks in K and

Table 5.1: Eigenvalues and variances of PCA before and after Varimax rotation.

PC	initial eigenvalues			squared loadings after rotation		
	total	% of variance	cumulated %	total	% of variance	cumulated %
1	5.830	64.777	64.777	5.319	59.096	59.096
2	1.292	14.352	79.129	1.678	18.643	77.739
3	0.943	10.480	89.609	1.068	11.870	89.609
4	0.510	5.665	95.273			
5	0.211	2.343	97.617			
6	0.128	1.427	99.044			
7	0.053	0.591	99.635			
8	0.023	0.252	99.886			
9	0.010	0.114	100.000			

Mg. Na and PO_4 concentrations are placed together in one group as both feature a trend throughout the profile. Na has low values of 0.5 mg/g at the base of the core and then escalates to 1.5 mg/g at 590 cm depth. From here a relatively continuous decrease towards 0.5 mg/g in the upper part of the core is only intermitted by two outliers at 170 and 490 cm depth. PO_4 also shows low concentrations (approx. 1 mg/g) at the base of the sediment core. Following an erratic increase at 590 cm depth the curve is characterized by a slightly increasing trend from bottom to top.

5.4.4 Principal Components

In order to reduce the complexity of the sediment's chemical character, PCs were extracted from the data described above. As the underlying 30 cm of the core reflect a fluvial depositional environment PC analysis was restricted to the core section above 600 cm depth. The variables included in the PCA are Ca, Fe, K, Mg, Mn, S, Sr, TIC and TOC. The heavy metals Cr, Cu, Ni and Pb were excluded due to the strong noise associated with their relatively low concentrations close to the detection limit. Na and PO_4 were debared because they have shown to load on a separate factor due to their trend behaviour.

Three factors explain 89.6% of the variance of the variables included in the PCA. After Varimax rotation 59.1% are attributed to the first, 18.6% to the second and 11.9% to the third PC (table 5.1). The proportions of each variable's variance explained by the extracted PCs (communalities) are listed in table 5.2.

Table 5.2: Factor loadings (eigenvectors) and communalities of log-ratio transformed variables after Varimax rotation.

element	factor loading			communality
	PC1	PC2	PC3	
Mg	**-0.970**	-0.081	-0.041	0.950
Fe	**-0.947**	-0.214	0.054	0.946
K	**-0.928**	-0.231	-0.089	0.923
TIC	**0.882**	0.262	-0.181	0.879
Ca	**0.852**	0.461	-0.105	0.950
Sr	**0.752**	0.574	-0.092	0.903
S	**0.727**	-0.332	0.145	0.660
Mn	0.144	**0.923**	-0.012	0.872
TOC	-0.008	-0.031	**0.991**	0.983

The variables are rather distinctly allocated to the PCs. PC1 is associated with TIC, Ca, Fe, K, Mg, S and Sr, whereby Fe, K and Mg are negatively correlated with PC1. PC2 describes 85% of the variance of Mn and a minor part of the variance of Sr can be attributed to this factor. Strong correlation of PC3 solely exists with TOC.

5.4.5 Minerals

Mineral composition comprises the allogenic and authigenic mineral fraction (Fig. 5.5). Allogenic minerals constitute the major portion of all samples with a dominance of quartz and feldspars. Semi-quantitatively determined proportions of quartz and feldspars range between 46 and 94 vol.-% with a median of 91 vol.-% for all samples. A differentiation of the feldspar group yields mainly polymorphs of alkali feldspars (orthoclase, sanidine and microcline) and the end-member albite. Further silicates detected as traces are chlorite, hornblende, kaolinite and muscovite.

Calcite is found in 23 samples with concentrations ranging from 1 to 37 vol.-%. Pyrite and gypsum could be identified in several samples albeit only as traces. Occurrences of pyrite and gypsum are predominantly restricted to the lower and middle part of the profile (Fig. 5.5) and are mostly associated with calcite. Monohydrocalcite (MHC) is found in two samples in 160 and 310 cm depth. While in latter sample MHC only vestigially occurs, its proportion in the 160 cm sample is higher than 20 vol.-%.

5.5 Discussion

5.5.1 Element and mineral composition

Interpretation of principal components

Element and mineral compositions vary in the Ugii Nuur lake sediments. The PCA on the log-ratio transformed element compositions depicts that their variance is basically explained by one factor. Positive loadings on PC1 exist with TIC, Ca, Sr and S; elements that mainly reflect the authigenic mineral production in the lake. Positive values of PC1 are consequently interpreted to reflect warm limnic conditions and high biomass production in the lake. This interpretation is based on several aspects. The authigenic production of TIC is subject to various physical lake conditions (temperature, CO_2, solute concentration) that are partly linked to biomass production (Håkanson and Jansson, 1983; Dean, 1999; Xiao *et al.*, 2006). Optimal conditions for the incorporation of endogenic carbonate minerals in sediments are derived from a combination of these parameters. The water temperature of shallow lakes in summer is generally high and the water body is unstratified due to a lack of sufficient depth to form a hypolimnion in summer, and thus promotes calcite sedimentation. Calcite solubility is further decreased by increasing pH values during algal blooms (Dean, 1999).

Increased biological activity, however, simultaneously leads to an increase of respiratory CO_2 production. This inverse effect on carbonate solubility is presumably buffered by allogenic contribution of calcite to the lake (Håkanson and Jansson, 1983). Due to an absence of carbonate rocks in the Ugii Nuur catchment the input of calcite derived from bedrock solution can be excluded. Yet, it was shown by Lehmkuhl and Lang (2001) and Grunert and Lehmkuhl (2004) that carbonatic loess-like deposition plays an important role in the sediment budget of the Mongolian steppe regions. Direct aeolian deposition in the lake and input of calcium carbonate or its solutes by removal of aeolian deposits by water erosion may be an important carbonate source for lacustrine carbonate precipitation. Moreover, the proportion of allogenic calcite in the lake is linked to the lake volume. The assumption of a decreased lake volume during high values of PC1 is further consolidated by a preponderant cooccurrence of authigenic minerals like pyrite and gypsum (Fig. 5.5).

While sulfides are formed under highly reduced conditions and thus indicate productive lakes (Håkanson and Jansson, 1983), sulfates are primarily precipitated from solutions with densities higher 1.115 g/cm^3 and thus indicate increased salinity driven by evaporation (Langbein, 1961; Sonnenfeld, 1984; Schütt, 2004b).

The elements K, Mg and Fe negatively relate to PC1 and are interpreted as lithogenous or allogenic sediment fraction. Despite the removal of possible dilution effects on the data by log-ratio transformation, the diametrical behaviour between authigenic and allogenic sediments remains. Thus, negative values of PC1 are related to high lake levels and increased detrital input. The results from the upper part of the sediment core reflect this situation and are confirmed by the current state of the water body that is characterized as oligo- to mesotrophic and thermally stratified (Völker, 2005). Higher lake levels than present are exspected to exceed the present state by a maximum of only two meters due to a lack of damming in the west of the basin and a consequent overflow to the Orkhon River (Fig. 5.1).

Mn variability is assigned to an independent mechanism described by PC2. Mn in lacustrine sediments is sensitive to lake and catchment conditions and is often compared to Fe by means of the Fe-Mn ratio (Mackereth, 1966; Boyle, 2001; Schütt, 2004b). A comparison of Fe and the Fe-Mn ratio (Fig. 5.4) reveals that the relation between both elements varies along the core. While in the upper part Fe and the Fe-Mn ratio graphs exhibit an opposing course, parallel behavior prevails in the lower part of the core. As aforementioned, Fe is related to the lithogenous sediment fraction, which indicates a strong erosional mode of transport of this element (Hartmann and Wünnemann, 2007). The parallel course of Fe and Mn in the upper part of the core is characterized by high Fe and low Mn concentrations in comparison to the concentration range of both. Mn concentrations during this phase presumably equal those of the lithospheric background (Mackereth, 1966). The underlying part of the core (>160 cm depth, >2.8 ky BP) is characterized by much stronger fluctuations of both elements. Sharp increases in Mn contents are always accompanied by negative Fe-concentrations. As low contents of Fe indicate an attenuation of the lithogenic sediment fraction, the correlative high contents of Mn point towards a different source of Mn. We suggest that these phases are marked by low allothigenic input by surface

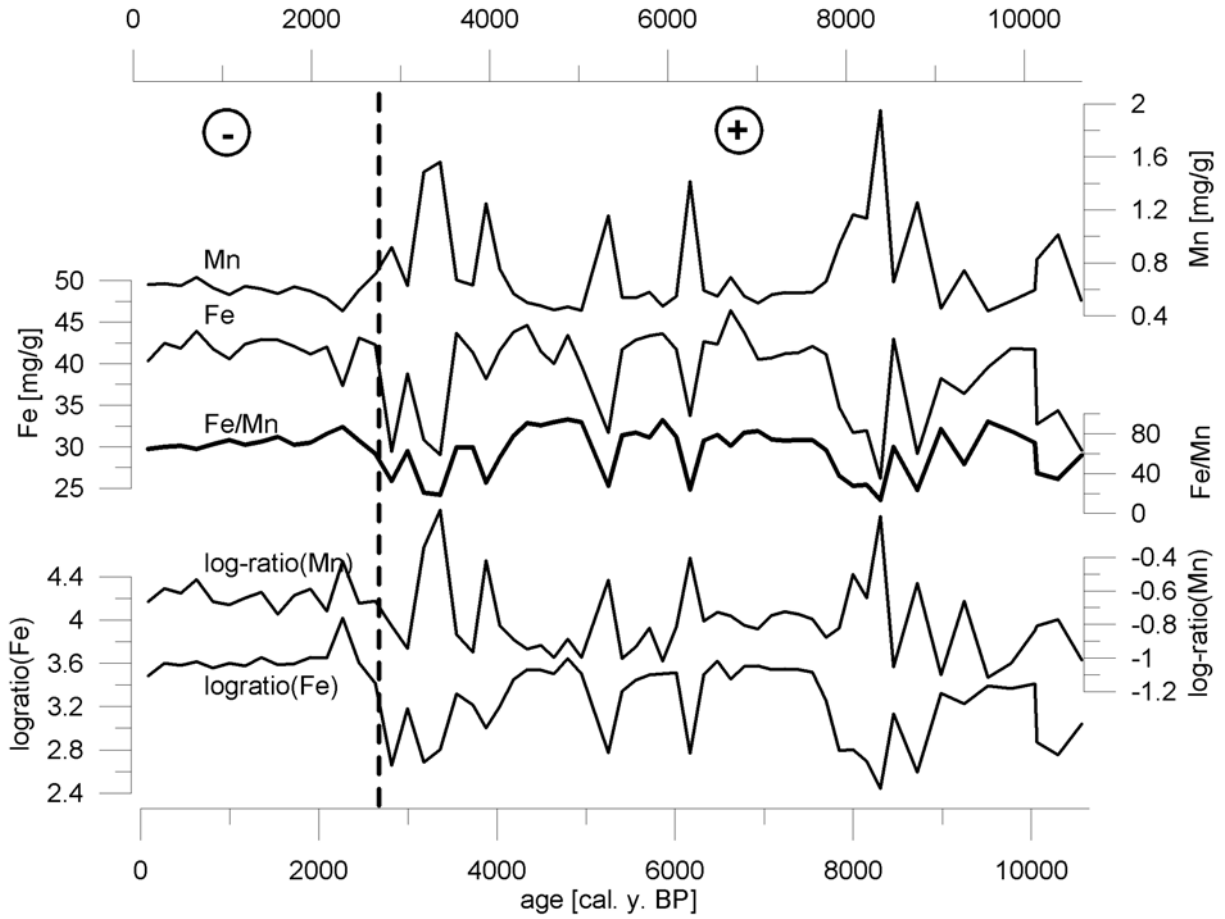

Figure 5.4: Compositional and log-ratio transformed Fe, Mn and Fe-Mn ratio. Minus signs point at section in the core with negative correlation of Fe and the Fe-Mn ratio, and vice versa.

runoff and that the lake is predominantly fed by groundwater. Since Mn in soils is more easily mobilized than iron under reducing conditions (Schlichting and Schweikle, 1980), groundwater is enriched in dissolved Mn, which is subsequently incorporated in the lake sediments. This assumption is consolidated by the medium PC2 loadings of Ca and Sr (table 2), that are highly mobile in soils, too (Scheffer, 2002). As a consequence we interpret PC2 to reflect solute transport from the catchment via groundwater into the lake. A positive trend of PC2 thus indicates aquifer filling and soil formation during the Holocene.

PC3 reflects the mechanism behind TOC accumulation in the lake sediments. TOC enrichment can be attributed to increased autochthonous bioproduction, dedrital input from the catchment (Dunne *et al.*, 1991; Boyle, 2001; Xiao *et al.*, 2006) and preservation,

when covering rates exceed diagenetic decomposition rates (Lerman, 1979; Schütt, 2004a). These diverse mechanisms impede paleoclimatological interpretations inferred from TOC concentrations without additional source signals (e.g. N, δ^{13}C) (Meyers, 1994; Xiao *et al.*, 2006; Hartmann and Wünnemann, 2007). Still, various correlative peaks of TIC and TOC suggest a synsedimentary mechanism during some periods. Since TIC is interpreted to negatively correspond with waterdepth, TOC concentrations during low lakel levels may largely reflect increased biological productivity (Scheffer, 2004). Yet, relatively high TOC concentrations ($\sim$ 2)%) prevalent during high lake levels suggest the additional influence of terrestrial organic matter (plant detritals, humins) transported to lake via groundwater or overland flow (Xiao *et al.*, 2006).

Monohydrocalcite

A rather rare mineral found in 160 and 310 cm depth is MHC ($CaC0_3 \cdot H_2O$). The natural occurrence of this hydrated calcium carbonate was first reported by Sapozhnikov and Tsvetkov (1959) in form of calcareous incrustations on the bottom near the shore of Lake Issyk-Kul, Kirgistan. It has been found by Marschner (1969) at the mouths of cold water pipes, by Taylor (1975) as a main constituent in beach rocks in southern Australia and by Fischbeck and Müller (1971) and Harmon (1983) in speleothems. A marine occurrence of MHC has been first reported by Dahl and Buchardt (2006) for south-west Greenland.

MHC formation is attributed to several mechanisms. Laboratory experiments suggest a preferable MHC genesis at water temperatures near the freezing point (Lippmann, 1973) and natural occurrences have often been associated with cold water (Marschner, 1969; Fischbeck and Müller, 1971; Harmon, 1983). Yet, biological activity is also regarded as an important mechanism behind MHC formation (Broughton, 1972; Taylor, 1975; Skinner *et al.*, 1977). Since it was shown that MHC tends to convert to anhydrous carbonates even at low termperatures (several authors in Lippmann, 1973) a stable basis for the interpretation of MHC as proxy for lake temperatures is lacking.

Paleoenvironmental implications

Datings point to an onset of lacustrine sedimentation in the Ugii Nuur lake at 10.6 ky BP after a period of fluvial deposition most likely by the Orkhon or Old Orkhon River (Phase 1 (P1)) (Walther and Gegeensuvd, 2005). The temporal placement is in good agreement with other lakes in NW China and Mongolia that predominantly featured a negative water balance or were dried out during the Last Glacial Maximum (LGM) and the beginning of the Holocene (Grunert and Dasch, 2004; Hartmann and Wünnemann, 2007; Karabanov *et al.*, 2004; Tarasov *et al.*, 1999b; Walther, 1999; Walther *et al.*, 2003; Wünnemann *et al.*, 1998; Wünnemann and Hartmann, 2002; Yang *et al.*, 2004). Rapid increases in lake levels may be attributed to meltwater generated by the glacier retreat after the LGM (Walther, 1999). Yet, the occurrence of glaciers in the Ugii Nuur basin was limited to the higher regions of the Khangay mountains (Lehmkuhl *et al.*, 2004). Lake level rise may also be linked to the abrupt monsoon intensification at $\sim$ 11.5 ky BP (Sirocko *et al.*, 1993; Wang *et al.*, 1999; Herzschuh, 2006).

PC1 scores indicate a generally lower lake level than today with high biological productivity during the early phase of lake evolution from 10.6 to 7.9 ky BP (P2) (Fig. 5.5). Low values of PC3 point at efficient decomposition during the underlying half of this section but might also indicate a poor availability of organic matter from the catchment. The findings of gypsum, pyrite and generally low but partly moderate concentrations of calcite in this section support the notion of the high lake internal productivity, a lack of outflow and evaporation driven water balance during this time. From 10.1 to 9.1 ky BP PC1 values around zero point at a well-balanced ratio between deposition of authigenic and allogenic material during moderate lake levels. Lake desiccation from 9.1 to 7.9 ky BP is in good agreement with a marked dry phase observed in NW China and the Tibetan Plateau (Herzschuh, 2006; Wünnemann *et al.*, 2003; Xiao *et al.*, 2004; Hartmann and Wünnemann, 2007) and might be attributed to the 8.2 ky BP event (Alley and Agustsdottir, 2005). These results, however, disagree with evidences of wetter conditions in NW Mongolia inferred from the rise of boreal evergreen and conifer pollen since 9 ky BP (Tarasov *et al.*, 2000).

A subsequent phase of high lake levels interrupted by a period with pronounced fluc-

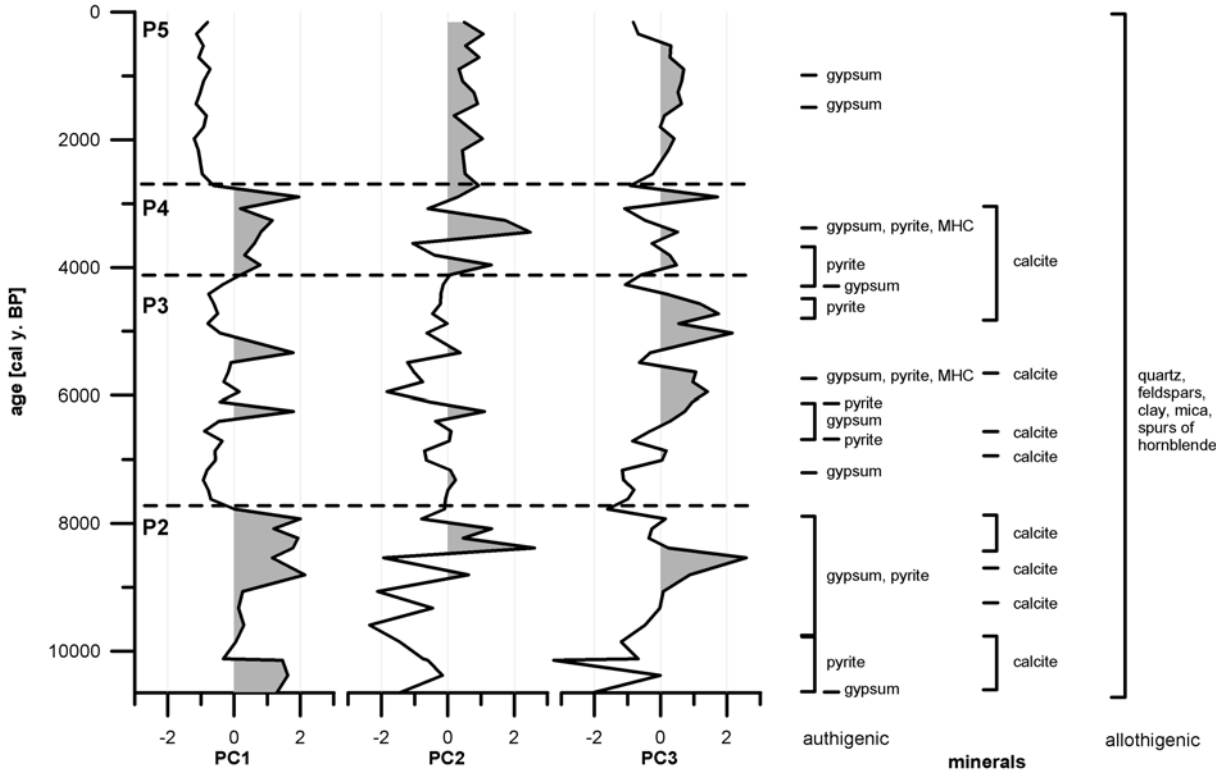

Figure 5.5: Chronology of principal components (PC) and occurrences of minerals.

tuations occurred from 7.9 to 4.2 ky BP (P3). During this time allogenic material is dominantly supplied to the lake bottom indicating increased runoff. Vegetation during this time was characterized by an increase in woodland (Rösch *et al.*, 2005). A marked increase in PC3 suggests the importance of detrital organic input and its poor decomposition during this period. In arid and semi-arid China most sites archive a relatively wet climate during the Mid Holocene (7–5 ky BP) (e.g. Xiao *et al.*, 2004, 2006) but spatial patterns among different lakes are inconsistent (An *et al.*, 2006; Hartmann and Wünnemann, 2007). High water levels are reported for most Mongolian lakes during the Mid-Holocene (Dorofeyuk and Tarasov, 1998; Grunert *et al.*, 2000; Tarasov *et al.*, 2000). Yet, Peck *et al.* (2002) and Fowell *et al.* (2003) indicate a Mid Holocene dry climate for Lake Telmen. Corresponding to the irregular spatial pattern of moisture availability, the temporal lake level pattern as observed in P3 and the sporadic occurrences of pyrite and gypsum during this period reflect a rather unstable development of the lake during the Mid Holocene and a higher sampling rate is required to reliably resolve these fluctuations.

From 4.2 to 2.8 ky BP (P4) a phase of reduced lake levels is indicated by PC1. Constant calcite precipitation and occurrences of pyrite and gypsum suggest high biological activity and salinity of the lake water during this time. This period agrees fairly well with the temporal placement of a dry phase from 5.4 to 2.9 ky BP observed in Mongolia (Walther *et al.*, 2003) and northwest China (Xiao *et al.*, 2004) and correlates with a rapid decline of forest vegetation and a re-establishment of steppe as the dominant vegetation type in the Hoton-Nuur area at 4 ky BP (Tarasov *et al.*, 2000). Still, evidences for a more humid phase in Central Mongolia during this period are provided by Peck *et al.* (2002).

The Ugii Nuur record indicates stable high lake levels from 2.8 to present (P5), thus suggesting enhanced moisture supply during the Late Holocene. Although an onset of more humid conditions is reported during the beginning of the Late Holocene for areas in NW China and Mongolia (Hartmann and Wünnemann, 2007; Peck *et al.*, 2002; Walther *et al.*, 2003), evidence for a trend towards dryer conditions during the last three millenia is found in many parts of Central Asia except for those influenced by the westerlies (Herzschuh, 2006).

The chronology of the factor scores and their palaeoenvironmental interpretation partly agrees with previous findings from Central and East Asia. Nevertheless, they partly disagree with findings from other sites located relatively close to the Ugii Nuur basin (e.g. Lake Telmen (Peck *et al.*, 2002; Fowell *et al.*, 2003)). This highlights the problems associated with the ability to transfer the findings to a larger area and, thus, points at the difficulties that arise from the deduction of information on the general paleoenvironmental conditions. Spatially variable palaeoenvironmental conditions in NW China are mainly associated with the southward retreat of the South-East Asian Monsoon since 9 ky BP (An *et al.*, 2000) and the response of the Indian Monsoon and the westerlies (Herzschuh, 2006). Still, extreme differences exist among sites located close to each other (Herzschuh, 2006). Partly, the alternating timings of dry and wet intervals may be explained by site-specific sensitivities to moisture supply (An *et al.*, 2006). These site-specific sensitivities may be derived from the present aridity of a location (An *et al.*, 2006) but processes like aquifer response to moisture supply should also be taken into account (Hartmann and Wünnemann, 2007). Hence, in order to reduce the uncertainties associated with the interpretation of

lake sediments not only a larger quantity of lake proxies should be considered. Moreover, spatially distinct terrestrial archives should be investigated to understand catchment response to climate variability.

5.6 Conclusions and outlook

Lacustrine deposits of Lake Ugii Nuur provide valuable insights into the palaeoenvironmental evolution of the Ugii Nuur basin and the adjacent Orkhon Valley. During the Holocene the lake environment altered between open and closed lake conditions. Lacustrine deposition started at 10.6 ky BP. Low lake level conditions were identified during the Early Holocene (10.6–7.9 ky BP). It is proposed that lakes in this area benefitted from increased discharge induced by glacier melting in the Khangay Mountains during a warm but relatively arid period. The Mid Holocene (7.9–4.2 ky BP) was characterized by generally higher lake levels and thus increased moisture supply. Yet, this period was prone to strong climatic fluctuations. More arid conditions prevailed from 4.2–2.8 ky BP and were followed by a stable, more humid phase until today.

Archaeological findings provide evidences for the earliest human settlements in the Orkhon Valley more than two thousand years ($\sim$ 250 y BC) ago. Since then, the Orkhon Valley was a preferred settlement location of various cultures (Weiers, 2005). Remnants of walls, necropoles and memorials found all over the area testify this long history of human interference with the environment in this region (Bemmann *et al.*, 2008). A climax phase of human activities in this area represents the late Medieval, when Dschingis Khan chose the fan deposits of the Upper Orkhon Valley as locality for the Mongolian capital Karakorum (Qara Qorum). A question always was: Why was this area chosen again and again? We conclude, that, among many reasons, the three millenia lasting, favorable and stable environmental conditions in this area were at least an important factor.

Acknowledgements

We like to thank Dr. K. Hartmann from the Freie Universität Berlin for valuable discussions, E. Krings and Dr. H.-P. Röper for assistance in X-ray diffractometry and Joris Peters from LMU Munich for the identification of the fishscale.